High dielectric material dependence of carbon nanotube field effect transistor considering non-ballistic conduction

Nirjhor Tahmidur Rouf[1], Ashfaqul Haq Deep[2], Rusafa Binte Hassan[2], Sabbir Ahmed Khan[3], Mahmudul Hasan[2], Sharif Mohammad Mominuzzaman[4]

[1]*Control and Applications Research Centre, BRAC University, Dhaka 1212, Bangladesh*
[2]*Department of Electrical and Electronic Engineering, BRAC University, Dhaka 1212, Bangladesh*
[3]*BRACU Robotics Research Lab, School of Engineering and Computer Science, BRAC University, Dhaka 1212, Bangladesh*
[4]*Department of Electrical and Electronic Engineering, Bangladesh University of Engineering and Technology, Dhaka 1000, Bangladesh*
E-mail: rouf.t.nirjhor@gmail.com

Published in Micro & Nano Letters; Received on 16th May 2014; Accepted on 7th July 2014

As a result of this reported research, a simulation model to analyse the behaviour of carbon nanotube field effect transistors (CNTFETs) under non-ballistic conditions is explained and the effect of gate dielectric on the performance of CNTFETs has been explored in detail. For the first time, a thorough study of the combined non-ballistic effect on the performance of CNTFETs has been conducted and the output of the device has been analysed. It has been observed that a gate material with a high dielectric constant leads to higher on-state current and higher on and off state current ratio. In addition, the transconductance, total capacitance, charging energy, subthreshold swing (S), drain-induced barrier lowering (DIBL) and gain with respect to the dielectric constant have been observed and analysed. Transconductance and total capacitance increases by a significant amount, while charging energy and S decrease as the dielectric value increases. The DIBL and gain vary slightly as a higher value dielectric material is used as a gate. Furthermore, the results of this study have been plotted against previously reported ballistic outputs to provide a better perception of the deviation from ideal behaviour. At the same time, the outcomes of this analysis have been compared against some reported experimental values.

1. Introduction: At present, it is becoming increasingly difficult for researchers to comply with the demands of Moore's Law and the International Technology Roadmap for Semiconductors (ITRS) with the on hand silicon technology because of various material issues and scaling limitations, such as gate thickness, parasitic resistance, short channel effect and so on [1]. These complications have compelled scientists to search for new materials which may be used to upgrade the present-day technology. Following the invention by Iijima [2], carbon nanotubes (CNTs) have aroused the curiosity of many researchers as a potential candidate to be used in field effect transistor (FET) technology because of its excellent mechanical [3] and electrical properties [4, 5]. Several researches have already been carried out to analyse the performance of CNTFETs under various conditions [6–18]. Natori has already reported the higher on-state current in carbon nanotube field effect transistors (CNTFETs) compared with the traditional metal oxide semiconductor field effect transistor (MOSFET) because of high channel density and high electric density [19]. Furthermore, scaling of present-day MOSFETs being restricted by gate oxide thickness [1] has widened the scope of CNTFETs. Concurrently, it has been observed that gate oxide thickness maintains an inverse relationship with the drain current of CNTFETs [7, 10, 20]. To tackle the constraint imposed on the scaling of FETs by gate thickness, researchers have proposed multiple solutions over the years and one of the most practical of these is using a material with a higher dielectric constant (k) as the gate [11, 21–23]. The effects of high-k material on the performance of CNTFETs considering the ballistic conduction has already been scrutinised and positive outputs have been recorded [6, 24, 25].

The novel work reported in this letter explored the variation in the current–voltage (I–V) characteristics of a MOSFET-like CNTFET considering the non-ballistic conduction for different dielectric constants. In this research we chose non-ballistic over ballistic conduction because physical strain, mismatch of helicity between adjacent shells, vacancies, contamination, contact with substrates and so on may result in non-ballistic transport [26]. These reasons contribute to the possibility that, in reality, non-ballistic transport may preside over ballistic conduction in CNTFETs. The non-ballistic effects considered for this experiment are the elastic scattering effect, the bandgap strain effect and the tunnelling effect. In addition, I_{on}/I_{off}, transconductance, total capacitance, charging energy, subthreshold swing, gain and drain-induced barrier lowering (DIBL) have also been analysed to achieve a better understanding of non-ballistic effects. Moreover, the simulation results are matched with previously reported experimental values to perceive the performance deviation of the considered CNTFET from real-world standards.

The simulation model used in this study is detailed in Section 2 and the results are discussed in Section 3. Section 4 summarises the whole work and discusses prospective future work on this topic.

2. Methodology: The device considered for this simulation is a MOSFET-like CNTFET. The drain and source terminals are heavily doped in this structure. The operating principle of this device is based on the modulation of barrier height by gate voltage application and therefore the drain current depends on the number of charges induced in the channel by the gate voltage.

The original ballistic simulation model was developed earlier [27]. The model used for the purpose of this research has been modified using non-ballistic equations [28]. Moreover, a multiple parameter approach simulation model was used for this research [29].

Elastic scattering is almost completely dependent on the channel length of the CNTFET and the mean free path (MFP). The channel resistance is affected because of elastic scattering and this in turn lowers the applied drain voltage (V_{DS}). Therefore, the FET operates on a modified lower voltage, V_{DSeff} [28]

$$V_{DSeff} = \frac{L}{L + (d/d_0)\lambda_{eff}} V_{DS} \tag{1}$$

Here, the channel length is L, the diameter is d and d_0 is the reference

doi: 10.1049/mnl.2014.0268

diameter with a value of 1.5 nm [30]. λ_{eff} denotes the elastic scattering MFP, the value of which is taken to be about 200 nm [31].

In addition, it has been reported that the transport properties of a CNT is dependent on physical strain [32]. When subjected to strain, the CNT bandgap is tuned and the effective bandgap is different from the actual bandgap [28]. The new bandgap can be calculated using [28]

$$E_{\text{geff}} = E_{\text{g}} + \frac{\text{d}E_{g\text{strain}}}{\text{d}\chi}\chi \tag{2}$$

where E_{g} is the actual bandgap and E_{geff} is the tuned bandgap in (2). $\text{d}E_{\text{gstrain}}$ is the shift of the bandgap because of strain and χ is the distortion factor because of strain with a value of 0.1 [28].

The rate of change of the bandgap can be calculated using the following formula [28]

$$\frac{\text{d}E_{g\text{strain}}}{\text{d}\chi} = 3\sigma(1 + r_0)\text{sign}(2p+1)\cos(3\phi) \tag{3}$$

In (3), σ is the overlap integral of the tight-binding C–C model and it has a value of 2.7 [28]. r_0 is the Poisson's ratio and for this research, $r_0 = 0.2$ [28]. p can be obtained using $n - m = 3l - p$, where n and m are chiral indices. ϕ is the chiral angle and for a (n, m) CNT, its value can be determined by [33]

$$\phi = \tan^{-1}\left(\frac{\sqrt{a}m}{m + 2n}\right) \tag{4}$$

The effect of tunnelling is calculated using a two-step method. In this way, at first, a parameter called tunnelling probability (T_{t}) is introduced. When m^* is the effective mass [34], q is the charge of the electron, $\hbar$ is the reduced Planck's constant and T_{t} is given by [28]

$$T_{\text{t}} = \frac{\pi^2}{9}\text{e}^{-\left(\pi\sqrt{m*E_g^2}/\sqrt{8}qhF\right)} \tag{5}$$

The entity F in (5) is termed the tunnel control parameter. This parameter ultimately sets off tunnelling under a high electric field [28]. Several values of F have been computed and have been found to be in the range of 10^{36}. For simplification purposes, this work uses an average constant value of 9.798×10^{36} for F rather than using it as a variable. The tunnelling current can be computed using [28]

$$I_{\text{t}} = \frac{4qkT}{h}T_{\text{t}}\left[\text{In}\left(1 + \text{e}^{(qV_{\text{DSeff}} - E_{\text{geff}}/2 - E_{\text{F}})/K_{\text{B}}T}\right) - I_1\right] \tag{6}$$

where

$$I_1 = \text{In}\left(1 + \text{e}^{(qV_{\text{DSeff}} - E_{\text{F}})/K_{\text{B}}T}\right) \tag{7}$$

where E_{F} is the Fermi level and K_{B} is the Boltzmann constant in the equations. The tunnelling current lowers the self-consistent potential at the top of the barrier. This affects the threshold characteristics of the transistor. Hence, even though the tunnelling current increases the drain current by some amount, it is not at all advantageous for the performance of the device.

In the used simulation model, the drain current at a certain gate and drain voltage is calculated from the total charge that occupies the first subband in the nanotube [24, 27]. The method to calculate the drain current of a CNTFET with non-ballistic conduction has been modified from the ballistic model [27]. The steps are summarised as follows:

1. A value for V_G, V_{DS} and E_{F_1} are to be considered. For simplicity, V_S is grounded as potential reference.
2. The rate of change of bandgap with strain is calculated to calculate the tuned bandgap.
3. The modified drain voltage is to be calculated.
4. The total charge on the nanotube channel is computed. The charge at the top of the barrier is determined from the contributions from the source and the drain with the formulae

$$N_1 = \frac{D(E)}{2}\int_{-\infty}^{\infty} f(E + U_{\text{scf}} - E_{\text{F}_1})\,\text{d}E \tag{8}$$

$$N_2 = \frac{D(E)}{2}\int_{-\infty}^{\infty} f(E + U_{\text{scf}} - E_{\text{F}_2})\,\text{d}E \tag{9}$$

In (8) and (9), N_1 and N_2 are the positive velocity states filled by the source and the drain, respectively, $D(E)$ is the density of states, E_{F_1} and E_{F_2} are the source and drain Fermi levels correspondingly and U_{scf} is the self-consistent potential. To simplify the calculation, E_{F_1} is taken to be 0 and $E_{\text{F}_2} = -qV_{\text{DS}}$, where q is the electronic charge.
5. The self-consistent potential is to be determined to calculate the charge density at the top of the barrier. U_{scf} is found by adding the Laplace potential and potential because of mobile charge density. The potential because of mobile charge is given by

$$U_p = \frac{q^2}{C\sum}(N_1 + N_2) - N_0 \tag{10}$$

N_0 is given by

$$N_0 = \int_{-\infty}^{\infty} D(E)f(E - E_P)\text{d}E \tag{11}$$

The laplace potential can be obtained by

$$U_L = -q(\alpha_G V_g + \alpha_D v_D + \alpha_S V_S) \tag{12}$$

where

$$\alpha_G = \frac{C_G}{C\sum}, \quad \alpha_D = \frac{C_D}{C\sum}, \quad \alpha_S = \frac{C_S}{C\sum} \tag{13}$$

6. Tunnelling probability is calculated to determine the tunnelling current (I_{t}).
7. The drain current is calculated using

$$I_{\text{D}} = \frac{4qk_{\text{B}}T}{h}\left[\text{In}(1 + \exp(E_{\text{F}_1} - U_{\text{scf}})) - \text{In}(1 + \exp(E_{\text{F}_2} - U_{\text{scf}}))\right] \tag{14}$$

8. The total drain current is computed by adding I_{t} and I_{D}.

The modified flow diagram of the simulation model used for this research is given in Fig. 1.

3. Results and analysis: This research considered a (13, 0) zigzag CNT with a bandgap of ~0.83 eV and a diameter of 1.0184 nm. A coaxial gate, separated by an oxide thickness of 1.5 nm, was placed around the intrinsic part of the nanotube. For the simulation, the temperature was set at 300 K. The gate and drain control parameters were 0.88 and 0.035, respectively. In addition to these, the source Fermi level was chosen to be −0.32 eV. These parameters were kept constant throughout the investigation. To plot the I–V curves, the gate and drain voltages were both been varied from 0 to 0.6 V.

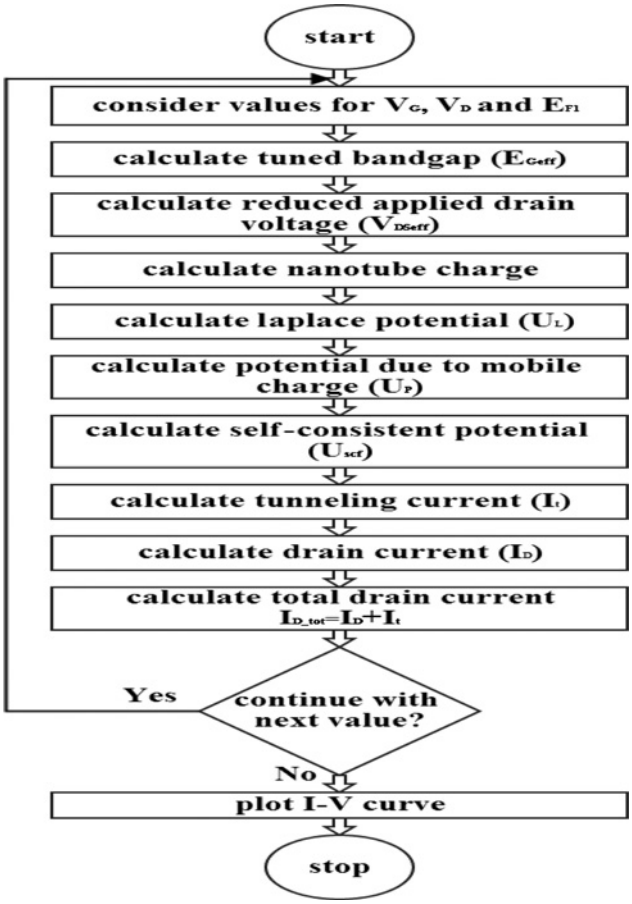

Figure 1 *Flow diagram used to calculate the drain current of CNTFET and plot the I–V curve*

In the current work, the dielectric constant has been changed from 3.9 to 30. Table 1 lists the gate materials considered for this research.

Fig. 2 presents a three-dimensional (3D) view of the change trend of the *I–V* characteristics of the CNTFET with respect to the dielectric constant. Previous researches on CNTFETs with ballistic conduction [6, 11] have shown that high dielectric materials wield a positive influence on the output of the device. This claim can be corroborated from the result of this work on non-ballistic conduction. The value of k has been varied from 3.9 to 30 with intervals of 1. It can be seen from Fig. 2 that the current increases sharply for the initial values of the dielectric constant and does so until $k \simeq 10$. Then the current starts to enter the saturation region and the rate of change of drain current decreases. Therefore, it can be deduced that increasing k continuously does not necessarily improve the current output of the CNTFET at the same rate.

Fig. 3 features the comparison of the ballistic *I–V* curves acquired from the CNTFETToy simulation tool [35]. The plot provides a comparative view of the current–voltage relationship for different

Table 1 List of gate dielectrics [38]

Name of gate dielectric material	Chemical formula	Dielectric constant
silicon dioxide	SiO_2	3.9
aluminium oxide	Al_2O_3	9
hafnium silicate	$HfSiO_4$	11
hafnium oxide	HfO_2	25
zirconium oxide	ZrO_2	25
lanthanum oxide	La_2O_3	30

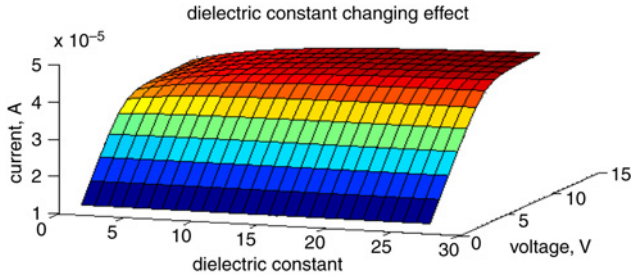

Figure 2 *3D view of the change trend of current–voltage relationship of CNTFET with non-ballistic conduction with respect to increasing dielectric constant*

dielectric materials. The curves have been plotted for a gate voltage of 0.6 V and the drain voltage has been changed from 0 to 0.6 V. Curves have been plotted for the listed materials. The graph presents the drain current of SiO_2 for both ballistic and non-ballistic conduction. The superiority of ballistic conduction can be clearly seen from the plot. Non-ballistic effects have reduced the output by almost 30% from the ballistic result. However, from the presented results it can be concluded that k maintains a positive relationship with the drain current output of the CNTFET for both ballistic and non-ballistic conduction.

Fig. 4, displays the ballistic output as reported in [6] by running the simulation under similar conditions. The sharp change rate of ballistic current can easily be noticed. On comparing with the non-ballistic change rate as shown in Fig. 2, it can be safely inferred that the ballistic rate of change of drain current of CNTFET is much more rapid than the non-ballistic change rate.

Fig. 5 reports a very important aspect of the transistor, the change in I_{on}/I_{off} with the dielectric constant. At the same time, it compares the on and off state current ratio for non-ballistic conduction with previously reported ballistic values. I_{off} has been measured for 0 V gate and 0.6 V drain voltage while for I_{on}, the gate voltage was 0.6 V and the drain voltage remained the same. From Fig. 5, it can be seen that the dielectric constant influences the I_{on}/I_{off} in a positive way and thus provides superior gate voltage control over the channel. This helps to reduce the off state current and the transistor moves towards ideal behaviour. However, the I_{on}/I_{off} is in the range of 10^5 for ballistic conduction [6, 12, 24], whereas, as seen from the plot, for non-ballistic conduction, using

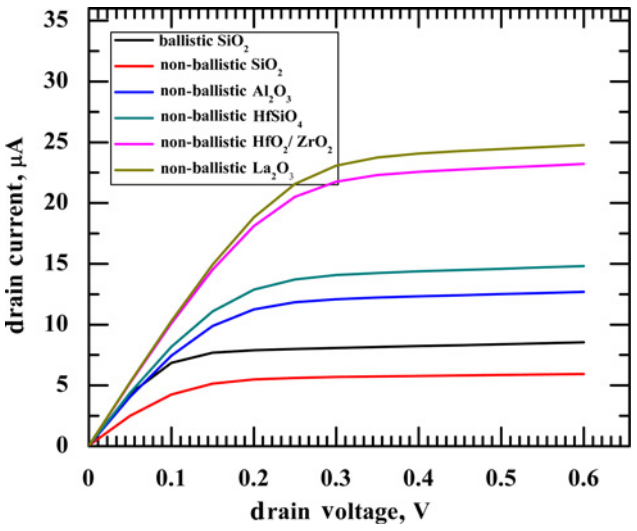

Figure 3 *Change effect of dielectric constant on the I–V characteristics of CNTFET for $V_g = 0.6$ V*

doi: 10.1049/mnl.2014.0268

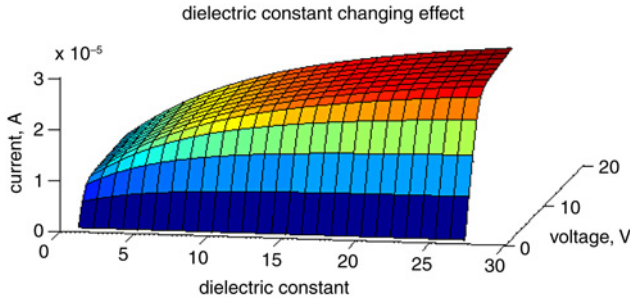

Figure 4 *Change trend of I–V characteristics of CNTFET with ballistic conduction with respect to dielectric constant*

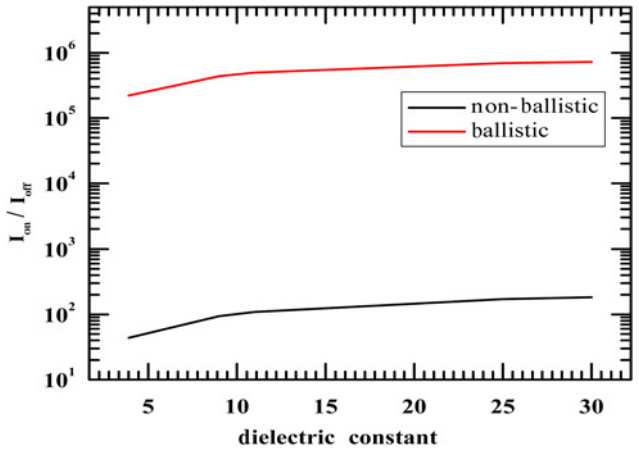

Figure 5 *Comparison of I_{on}/I_{off} of CNTFET with ballistic and non-ballistic conduction*

SiO_2 as the gate material results in an I_{on}/I_{off} of ∼44 which goes up to about ∼180 for La_2O_3. The effect of non-ballistic conduction can clearly be perceived from this data.

Fig. 6 plots transconductance against k. It is evident that transconductance rises with dielectric constant. As I_{on}/I_{off} goes up with k, on current also increases and so does transconductance. However, higher transconductance ensures that the FET provides a high I_{on} while maintaining the leakage current level. Fig. 6 also compares the non-ballistic transconductance with ballistic data and a slight deviation because of non-ballistic conduction from ideal behaviour can be observed.

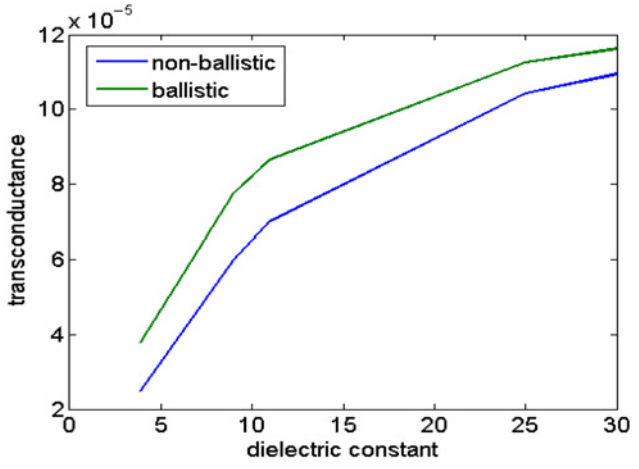

Figure 6 *Change effect of transconductance against dielectric constant for ballistic and non-ballistic conduction of CNTFET*

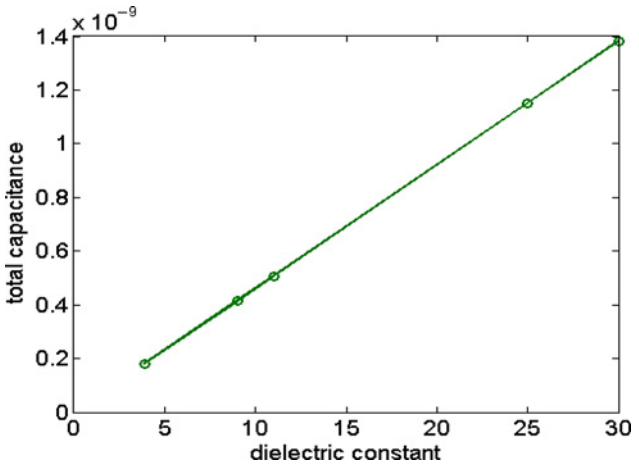

Figure 7 *Total capacitance against k*

Total capacitance and charging energy are given by [27]

$$C_{sum} = C_{ins}/\alpha_g \tag{15}$$

$$\text{Charging energy} = q^2/C_{sum} \tag{16}$$

Fig. 7 gives the change rate of total capacitance with respect to dielectric constant. It can be seen from the plot that the total capacitance increases with dielectric constant. This results in a decrease of switching speed of the FET. At the same time, charging energy decreases as total capacitance goes up, which affects the performance of the CNTFET in an adverse way.

Fig. 8 presents the relationship between charging energy and dielectric constant. Therefore, a higher charging energy or a lower total capacitance should be aimed for when designing the device.

The subthreshold swing (S) is an important factor regarding scaling. A small subthreshold swing is necessary to obtain a satisfactory value of I_{on}/I_{off}. Moreover, a low threshold voltage and low-power operation of small-sized FET depends on S. Theoretically S should be $(K_BT/e)\ln(10)$ or 60 mV/decade at room temperature. However, Fig. 9 shows that the subthreshold swing for non-ballistic conduction is quite high and ∼850 mV/decade and very far away from the ideal value. This explains the performance degradation for non-ballistic conduction. The plot also provides a comparison between non-ballistic and ballistic values of S. The ballistic value has also been calculated and is found to be ∼67, which is very near the theoretical value. It can also be concluded from the available data that the CNTFET with ballistic conduction operates very close to the ideal behaviour. Moreover, it can be said that non-ballistic effects cause the device to respond more slowly.

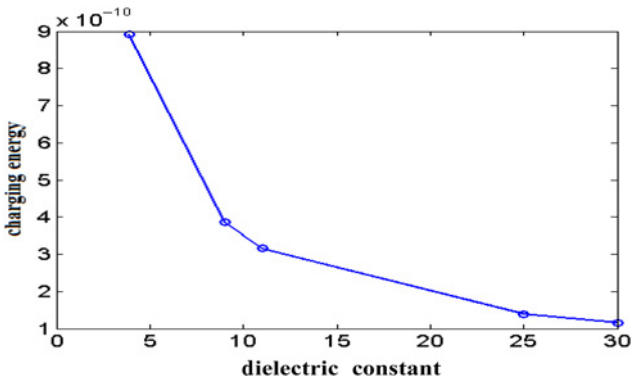

Figure 8 *Charging energy against k*

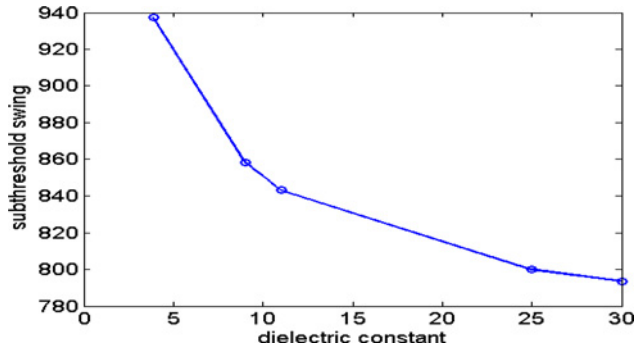

Figure 9 *Subthreshold swing against k for non-ballistic conduction*

DIBL is an electrostatic effect which is capable of changing the channel from pinch-off to conduction state and can result in a large leakage current. DIBL also lowers the threshold voltage and may turn on the device prematurely. This reduces the gate's control over the channel. For these reasons, circuits should be designed such that the DIBL effect can be countered [36]. DIBL occurs when, under the influence of high drain voltage, the drain electric field manipulates the barrier height for channel carriers at the edge of the source and decreases it. Fig. 10 shows that DIBL decreases, although slightly, with the increase of dielectric constant and thus puts the FET in an advantageous position. It also evaluates non-ballistic data against ballistic data. The DIBL for ballistic conduction is found to be ∼48 and also slightly decreasing. So, the DIBL effect is lower for non-ballistic conduction. Hence, the higher the k value, the better the performance of the CNTFET will be.

The gain is a function of transconductance (g_m) and drain conductance (g_d). Drain conductance is calculated from the on-state drain current. Therefore, a high gain may indicate a low g_d which may in turn be interpreted as a lower I_{on}. On the other hand, a high gain is better for amplification purposes. Fig. 11 shows the gain for non-ballistic conduction where the gain increases slightly with respect to the dielectric constant. The ballistic gain, which is about ∼24, has also been determined. The non-ballistic conduction provides a higher gain which actually is the result of a lower drain current.

This work also sought to evaluate the obtained simulation data against the experimental result of Javey *et al.* [37]. For a CNT with a diameter (d) of ∼1.6 nm and a bandgap of ∼55 eV and $E_F = -0.05$ eV, it was reported that the heavily doped CNTFET yields an I_{on}/I_{off} of 10^0 to 10^2. Under similar conditions, this simulation provides a value of ∼20. In addition, the on-current per unit width was computed to be ∼4400 μA/μm, which corresponds with the reported experimental value [37].

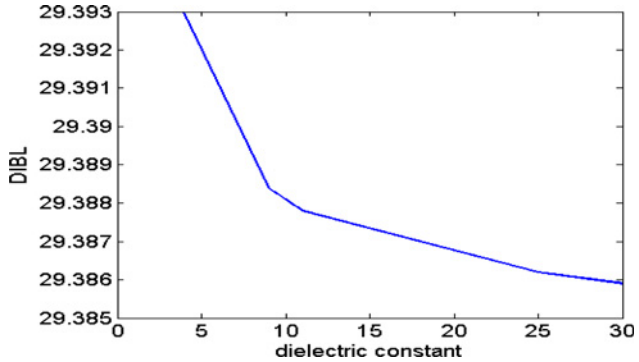

Figure 10 *DIBL against k for non-ballistic conduction*

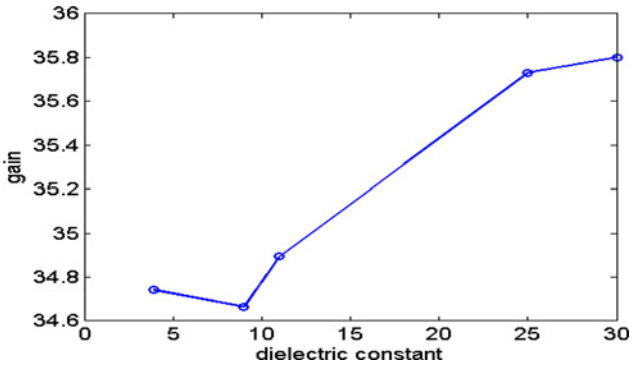

Figure 11 *Relationship between gain and k for non-ballistic conduction*

4. Conclusion: The effect of using different dielectric materials as the gate insulator on the performance of CNTFETs considering the non-ballistic conduction has been studied using a 2D and a 3D multiple parameter approach model. It has been realised that the value of k maintains a positive relationship with the performance of CNTFETs, by increasing the I_{on}/I_{off}, which leads to a higher on-state current. Besides, a higher k material provides better transconductance and maintains the level of leakage current. At the same time, a high-k material provides better gate control over the channel by reducing DIBL. The subthreshold swing is also decreased to improve device performance. However, an increase of total capacitance and a decrease of charging energy reduces the switching speed of the device and degrades device performance, whereas an increase in the gain is caused by a lower drain current. In addition, a comparison with the ballistic results provides a better perception of the non-ballistic effects. Finally, on analysing the effects, it can be said that the use of a high-k gate material reduces the non-ballistic effect and nudges CNTFET performance towards ideal behaviour.

5. Acknowledgments: The authors are grateful to the Department of Electrical and Electronic Engineering of both the BRAC University and Bangladesh University of Engineering and Technology that made this work possible.

6 References

[1] Plummer J.D., Griffin P.B.: 'Material and process limits in silicon VLSI technology', *Proc. IEEE*, 2001, **89**, (3), pp. 240–258
[2] Iijima S.: 'Helical microtubules of graphitic carbon', *Nature*, 1991, **354**, pp. 56–58
[3] Dresselhaus M.S., Dresselhaus G., Sugihara K., Spain I.L., Goldberg H.A.: 'Graphite fibers and filaments'. Springer Series in Material Science, Berlin, Germany, Springer, 1988, p. 5
[4] Ebbesen T.W.: 'Carbon Nanotubes'. American Institute of Physics, June 1996
[5] Seetharamappa J., Yellappa S., D'Souza F.: 'Carbon nanotubes: next generation of electronic materials', *Electrochem. Soc. Interface*, 2006, **15**, pp. 23–26
[6] Khan S.A., Hasan M., Alom Z., Mahmood S., Mominuzzaman S.M.: 'High dielectric material dependent current-voltage features of carbon nanotube field effect transistor'. Carbon, Brazil, 2013
[7] Khan S.A., Hasan M., Alom Z., Mahmood S., Mominuzzaman S.M.: 'Novel simulation approach to find the performance dependency of MOSFET-like CNFET on gate oxide thickness'. Carbon, Brazil, 2013
[8] Khan S.A., Hasan M., Alom Z., Mahmood S., Mominuzzaman S.M.: 'Temperature dependence of current–voltage (I–V) characteristics of carbon nanotube field effect transistor'. Carbon, Brazil, 2013
[9] Rouf N.T., Deep A.H., Hassan R.B., Khan S.A., Hasan M., Mominuzzaman S.M.: 'Current–voltage characteristics of non-ballistic CNTFET: effect of dielectric constant'. IEEE 2014 9th Int. Conf. on Nano/Micro Engineered and Molecular Systems (IEEE-NEMS), Hawaii, USA, April 2014

doi: 10.1049/mnl.2014.0268

[10] Rouf N.T., Deep A.H., Hassan R.B., Khan S.A., Hasan M., Mominuzzaman S.M.: 'Current–voltage characteristics of CNTFET considering non-ballistic conduction: effect of gate oxide thickness'. IEEE 2014 2nd Int. Conf. on Devices, Circuits and Systems (IEEE-ICDCS), Tamil Nadu, India, 6–8 March 2014, pp. 467–470
[11] Cheng B., Cao M., Rao R., Inani A., Voorde P.V., Greene W.M.: 'The impact of high-*k* gate dielectrics and metal gate electrodes on sub-100 nm MOSFETs', *IEEE Trans. Electron Devices*, 1999, **46**, pp. 1537–1544
[12] Arefinia Z., Orouji A.A.: 'Investigation of the novel attributes of a carbon nanotube FET with high-*k* gate dielectrics', *Phys. E*, 2008, **40**, pp. 3068–3071
[13] Hashim A.M., Ping H.H., Pin C.Y.: 'Characterization of MOSFET-like carbon nanotube field effect transistor'. American Institute of Physics, ICAMN, 2010, **1217**, (1), pp. 11–17
[14] Naderi A., Noorbakhsh M.S., Elahipanah H.: 'Temperature dependence of electrical characteristics of carbon nanotube field-effect transistors: a quantum simulation study', *J. Nanomater.*, 2012, **2012**
[15] Natori K.: 'Ballistic metal-oxide-semiconductor field effect transistor', *J. Appl. Phys.*, 1994, **76**, pp. 4879–4890
[16] Knoch J., Lengeler B., Appenzeller J.: 'Quantum simulations of an ultra-short channel single-gated *n*-MOSFET on SOI', *IEEE Trans. Electron Devices*, 2002, **49**, pp. 1212–1218
[17] Martel R., Schmidt T., Shea H.R., Hertel T., Avour P.: 'Single and multi-wall carbon nanotube field-effect transistors', *Appl. Phys. Lett.*, 1998, **73**, pp. 2447–2449
[18] Tans J., Verschueren A.R.M., Dekker C.: 'Room-temperature transistor based on a single carbon nanotube', *Nature*, 1998, **393**, pp. 49–52
[19] Natori K.: 'Characteristics of carbon nanotube field effect transistor analyzed as a ballistic nano-wire field effect transistor', *J. Appl. Phys.*, 2005, **97**, (3), pp. 240–258
[20] Chuan H.C.: 'Modeling and analysis of ballistic carbon nanotube field effect transistor (CNTFET) with quantum transport concept'. MS Thesis, 2007, University Technology Malaysia, Malaysia
[21] Mudanai S., Fan Y.Y., Ouyang Q.: 'Modelling of direct tunneling currents through gate dielectric stacks', *IEEE Trans. Electron Devices*, 2000, **47**, (10), pp. 1851–1857
[22] Sahoo R., Mishra R.R.: 'Carbon nanotube field effect transistor: basic characterization and effect of high dielectric material', *Int. J. Recent Trends Eng.*, 2009, **2**, (7), pp. 40–42
[23] Kawamoto A., Jameson J., Cho K., Dutton R.: 'Challenges for atomic scale modeling in alternative gate stack engineering', *IEEE Trans. Electron Devices*, 2000, **47**, (10), pp. 1787–1794
[24] Sanudin R.B.: 'Characterization of ballistic carbon nanotube field effect transistor'. M.S. Thesis, University Technology Malaysia, Malaysia, 2005
[25] Sze S.M.: 'Physics of semiconductor devices' (John Wiley & Sons, Inc., Hoboken, NJ, 1981)
[26] Zhou D.: 'Circuit level modeling and simulation of carbon nanotube devices'. Ph.D. dissertation, School of Electronics and Computer Science, University of Southampton, UK, 2010
[27] Rahman A., Guo J., Datta S., Lundstrom M.: 'Theory of ballistic nanotransistors', *IEEE Trans. Electron Devices.*, 2003, **50**, (9), pp. 1853–1864
[28] Kazmierski T.J., Zhou D., Al-Hashimi B.M., Ashburn P.: 'Numerically efficient modeling of CNT transistors with ballistic and non-ballistic effects for circuit simulation', *IEEE Trans. Nanotechnol.*, 2010, **9**, (1), pp. 99–107
[29] Khan S.A., Hasan M., Alom Z., Mahmood S., Mominuzzaman S.M.: 'A novel approach towards multiple parameters modeling of MOSFET-like carbon nanotube field effect transistor'. Carbon, Brazil, 2013
[30] Deng J., Wong H.S.P.: 'A compact spice model for carbon-nanotube field-effect transistors including nonidealities and Its application – Part II: full device model and circuit performance benchmarking', *IEEE Trans. Electron Devices*, 2007, **54**, (12), pp. 3195–3205
[31] Amlani I., Lewis J., Lee K., Zhang R., Deng J., Wong H.S.P.: 'First demonstration of AC gain from a single-walled carbon nanotube common-source amplifier'. Proc. Electron Devices Meeting, IEDM, 2006, pp. 559–562
[32] Minot E.D., Yaish Y., Sazonova V., Park J.Y., Brink M., McEuen P.L.: 'Tuning carbon nanotube bandgaps with strain', *Phys. Rev. Lett.*, 2003, **90**, (15), pp. 156401/1–156401/14
[33] O'Connel M.J.: 'Carbon nanotubes properties and applications' (Taylor and Francis Group, Boca Raton, FL, 2006)
[34] Deng J., Wong H.S.P.: 'A compact SPICE model for carbon-nanotube field-effect transistors including nonidealities and its application – Part I: Model of the intrinsic channel region', *IEEE Trans. Electron Devices*, 2007, **54**, (12), pp. 3186–3194
[35] Rahman A., Wang J., Guo J. *ET AL.*.: (2006, Feb. 14). Fettoy 2.0–On line tool. Available at: https://www.nanohub.org/resources/220
[36] Choi W.B., Bae E., Kang D., *ET AL.* 'Aligned carbon nanotubes for nanoelectronics', *Nanotechnology*, 2004, **15**, (10), pp. 512–516
[37] Javey A., Tu R., Farmer D.B., Guo J., Gordon R.G., Dai H.: 'High performance n-type carbon nanotube field-effect transistors with chemically doped contacts', *Nano Lett.*, 2005, **5**, (2), pp. 345–348
[38] Robertson J.: 'High dielectric constant oxides', *Eur. Phys. J. Appl. Phys.*, 2004, **28**, pp. 265–291